

The rupture plane of the 16 February 2022 M_w 6.2 Guatemala, intermediate depth earthquake

R. Yani-Quiyuch *, L. Asturias ¹, D. Castro ¹

¹Instituto Nacional de Sismología, Vulcanología, Meteorología e Hidrología, INSIVUMEH, Guatemala.

Author contributions: *Conceptualization:* R. Yani-Quiyuch, L. Asturias. *Software:* L. Asturias, D. Castro. *Formal Analysis:* R. Yani-Quiyuch, L. Asturias, D. Castro. *Writing - original draft:* R. Yani-Quiyuch, L. Asturias.

Abstract On 16 February 2022, an intermediate depth intraplate earthquake of M_w 6.2 struck the Guatemalan subduction zone with its epicenter located to the southwest of the department of Escuintla, along the Pacific coast. Following the main event, over 275 aftershocks were recorded and subsequently relocated using the HypoDD algorithm. This analysis revealed a fault with an area of ~ 350 km², significantly larger than what would typically be expected for an earthquake of this magnitude. The moment tensor at the centroid of the main earthquake, along with estimations of focal mechanisms for the largest aftershocks, enabled the identification of both normal earthquakes associated with the fault plane and inverse earthquakes linked to seismic activity in the upper part of the slab. Notably, the region where this seismic sequence occurred has experienced heightened seismic activity in recent years. We propose that the mainshock nucleated in the lower seismicity layer (LSL) of the region's double seismicity zone, subsequently triggering seismic activity on a pre-existing active fault, and also in the upper seismicity layer (USL). We estimate a separation of 12.2 ± 5.0 km between these two seismicity layers.

Resumen Un sismo intraplaca de profundidad intermedia con M_w 6.2 ocurrió en la zona de subducción guatemalteca el 16 de febrero de 2022, con epicentro en el suroeste del departamento de Escuintla, en la costa del Pacífico. Se registraron más de 275 réplicas, las cuales fueron relocalizadas con el algoritmo HypoDD, pudiendo identificar una falla con un área de ~ 350 km², la cual es considerablemente superior a la esperada para un sismo de esa magnitud. El tensor de momento en el centroide del sismo principal y la estimación de otros mecanismos focales de las réplicas más grandes, permitieron identificar sismos normales, relacionados al plano de falla y sismos inversos que fueron asociados a sismicidad en la zona superior del slab. La región de la secuencia ha presentado actividad sísmica alta en años recientes. Proponemos que el sismo principal nucleó en la capa inferior de sismicidad (CIS) de la zona doble de sismicidad de la región disparando actividad sísmica en una falla activa pre-existente y, además, en la capa superior de sismicidad (CSS). Estimamos una separación de 12.2 ± 5.0 km entre estas dos capas de sismicidad.

Non-technical summary On 16 February 2022, a magnitude 6.2 earthquake struck with its epicenter located in the department of Escuintla, on the Pacific coast of Guatemala. The earthquake occurred at an approximate depth of 70 km, within the Cocos plate as it subducts beneath the Caribbean plate. While the earthquake caused alarm among the population, only minor damage to some buildings was reported. Recent advancements in the Red Sismológica Nacional (RSN) enabled the registration of a significant number of aftershocks. This data allowed the identification of the fault plane associated with the earthquake and the activation of additional seismicity in the upper region of the same plate. Notably, the identified fault area is twice the size typically expected for an earthquake of this magnitude. Given the region's recent seismic activity, we propose that this earthquake and its aftershocks occurred along a pre-existing seismic fault. The detailed understanding of this seismic source, provided for the first time through instrumental means, allows for a better characterization of the hazard and seismic risk in Guatemala related to subduction earthquakes.

1 Introduction

On 16 February 2022, at 07:12 (UTC), a magnitude M_w 6.2 earthquake occurred in the subduction zone off the southern coast of Guatemala. The epicenter was situated in the department of Escuintla, near the department of Suchitepéquez (Figure 1). The seismic event had a depth of approximately 70 km and was felt by a sig-

nificant portion of the country's population. According to the Instituto Nacional de Sismología, Vulcanología, Meteorología e Hidrología (INSIVUMEH) instrumental measurements, seismic intensities of VI on the Modified Mercalli Intensity scale (MMI) were recorded. Due to the hypocenter's location and its normal focal mechanism, it was classified as an intraslab earthquake (Güendel and Protti, 1998; Alvarez, 2009; Guzmán-Speziale and Zúñiga, 2016; Guzmán-Speziale and Molina, 2022).

*Corresponding author: royani@insivumeh.gob.gt

Production Editor:
Gareth Funning
Handling Editor:
Marino Protti
Copy & Layout Editor:
Oliver Lamb

Signed reviewer(s):
Beatriz Cosenza-Murales

Received:
March 29, 2023
Accepted:
October 3, 2023
Published:
November 15, 2023

In recent years, the Red Sismológica Nacional (RSN) operated by INSIVUMEH (INSIVUMEH, 1976), has significantly expanded its number of seismic stations, equipped with velocity and acceleration sensors. Additionally, the Earthquake Early Warning in Central America (ATTAC) project, led by the Swiss Seismological Service (SED) at ETH Zurich in collaboration with Central American seismological agencies, has contributed further instrumentation provided by the Swiss Agency for Development and Cooperation (SDC). This network also includes stations donated by the Volcano Disaster Assistance Program (VDAP) of the US Geological Survey (USGS) for volcanic monitoring.

Moreover, INSIVUMEH benefits from real-time waveform data received from the Servicio Sismológico Nacional (SSN) of Mexico (SSN, 2022), the Ministerio de Ambiente y Recursos Naturales (MARN) of El Salvador (SNET, 2004), and the Comisión Permanente de Contingencias (COPECO) of Honduras (see Figure 1). These collaborative efforts have significantly improved hypocentral location accuracy and have opened up possibilities for conducting more detailed seismicity analyses in Guatemala and its surrounding regions.

In this paper, we utilize waveforms from a strengthened seismic network to conduct a detailed analysis of the earthquake that occurred on 16 February 2022, along with its subsequent sequence of aftershocks. By relocating the hypocenters, we successfully identified the rupture plane, which aligns with the moment tensor of the main earthquake and the normal focal mechanisms of certain aftershocks. Additionally, we discovered other earthquakes in the sequence, situated further away from the rupture plane, in the upper part of the slab, some of which exhibited an inverse focal mechanism. The analysis and interpretation procedure are described below.

2 The subducted Cocos Plate

Off the southern coast of Guatemala, the Cocos plate subducts under the Caribbean plate. This subduction zone gives rise to a significant number of earthquakes, which are monitored and recorded by the RSN. From southeastern Mexico to northwestern El Salvador (México-Guatemala-El Salvador Subduction Zone or MGESZ), the slab dip angle gradually changes from 20 to 60 degrees from the Middle America Trench to a depth of 280 km (Hayes et al., 2018), maintaining a relatively consistent overall shape (Hayes et al., 2018; Guzmán-Speziale and Zúñiga, 2016). The velocity of the Cocos plate with respect to the Central America forearc sliver to the northwest of MGESZ is 76.4 ± 2.5 mm/year, while to the southeast it is 75.0 ± 1.2 mm/year (Ellis et al., 2019) (Figure 1).

Historically, this subduction zone has been the source of several destructive earthquakes (e.g., Ambraseys and Adams, 1996; White et al., 2004; Ye et al., 2013; Ellis et al., 2018). Many of these events have been identified through both instrumental measurements and macroseismic observations, encompassing both interplate and intraplate regions (Ambraseys and Adams, 1996; White et al., 2004). Insights from centroid moment

tensors (CMTs) reveal a mix of inverse (compression) and normal (extension) focal mechanisms throughout the entire subduction process (Güendel and Protti, 1998; Alvarez, 2009; Guzmán-Speziale and Zúñiga, 2016; Guzmán-Speziale and Molina, 2022).

To observe the spatial distribution of subduction earthquakes and their focal mechanisms with better precision within MGESZ, we used the ISC-GEM catalog (Storchak et al., 2013, 2015; Di Giacomo et al., 2018), where it could be noticed that along the Middle America Trench, where the bending of the Cocos Plate still occurs at the onset of subduction, focal mechanisms are predominantly normal. In the interplate region (down to depths of around 40 km), focal mechanisms are mostly inverse, while at greater depths, a combination of both types of focal mechanisms is more commonly observed (Figure 1). This pattern mirrors the behavior seen in other subduction zones worldwide that possess relatively straightforward geometries (Craig et al., 2022).

The trigger mechanism of intermediate depth earthquakes is still a matter of debate. Among the most widely accepted explanations are dehydration embrittlement and the reactivation of previously formed faults within the outer rise region, faults initially generated during the plate bending process and subsequently reactivated during subduction (e.g., Ranero et al., 2005; Brudzinski et al., 2007; Kiser et al., 2011; Marot et al., 2012; Cabrera et al., 2021).

As observed in other global regions, detailed studies of intermediate-depth earthquakes have unveiled a double seismicity zone (DSZ) within the MGESZ slab. This DSZ is characterized by a separation between the upper seismicity layer (USL) and the lower seismicity layer (LSL) (Brudzinski et al., 2007; Florez and Prieto, 2019). In proximity to the earthquake of 16 February 2022, Brudzinski et al. (2007) noted a separation of 8.0 ± 6.6 km between USL and LSL, whereas Florez and Prieto (2019) reported a separation of 11.3 ± 4.0 km. This relatively small separation, compared to other subduction zones, is attributed to the youthful age of the subducting plate (Brudzinski et al., 2007; Florez and Prieto, 2019), which is estimated to be approximately 24 million years old (Nishikawa and Ide, 2014).

Brudzinski et al. (2007) found that, in the subduction zones they examined (without specific information about MGESZ) normal focal mechanisms were present in the LSL. On the other hand, earthquakes occurring at intermediate depths in the USL tend to exhibit inverse focal mechanisms (Craig et al., 2022; Chu and Beroza, 2022). Within the MGESZ, it has been estimated that normal earthquakes release more seismic moment than inverse earthquakes at these intermediate depths (Alvarez, 2009; Guzmán-Speziale and Zúñiga, 2016), this is consistent with other subduction zones in the world (Craig et al., 2022).

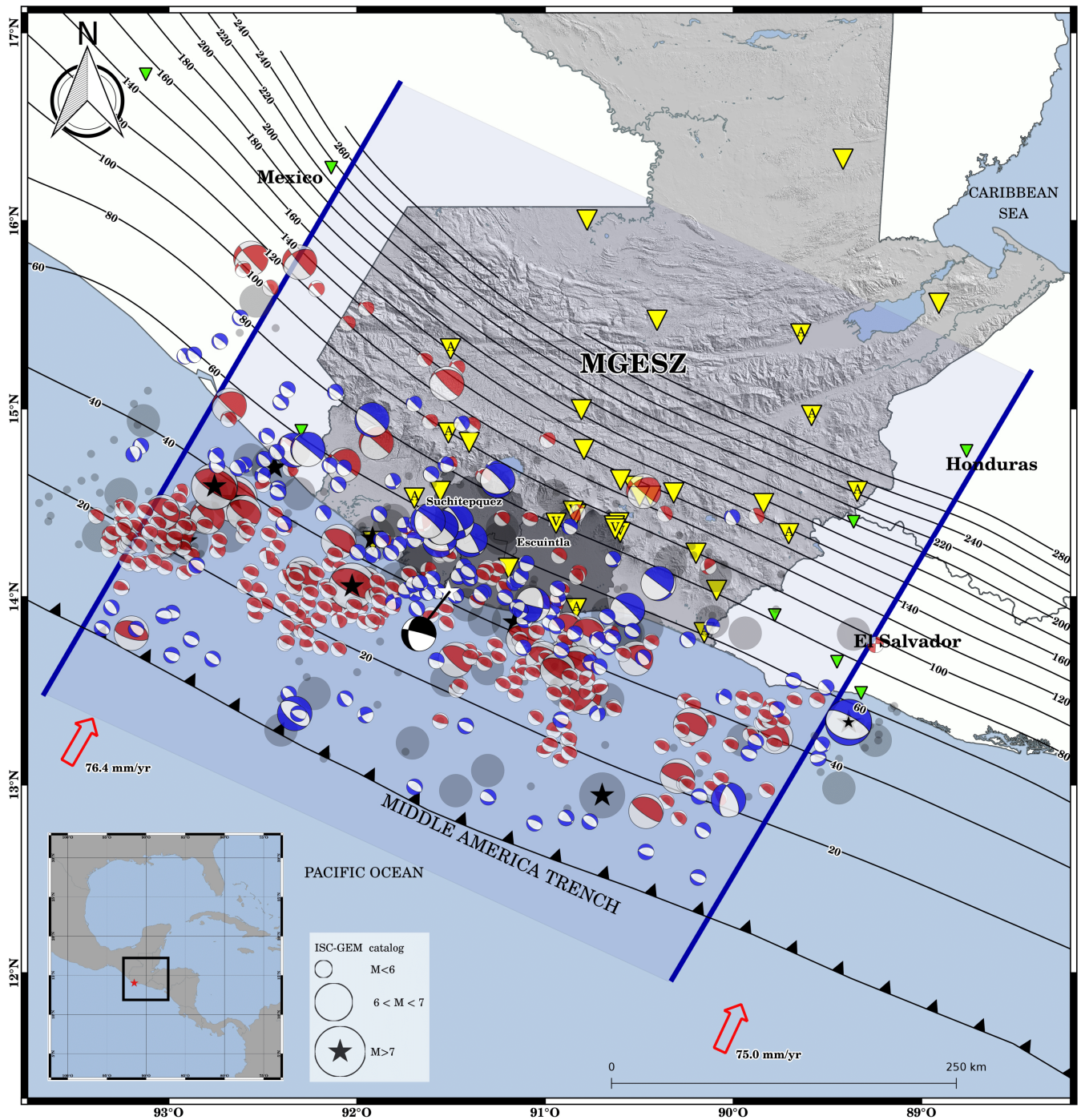


Figure 1 Subduction zone between the Cocos and Caribbean plates that includes the border with Mexico, Guatemala, and part of El Salvador (MGESZ). The iso-depth lines at the top of the slab (Hayes et al., 2018) indicate its relatively uniform shape. The preliminary epicenter of the 16 February 2022 earthquake is marked with a white star, and its focal mechanism is shown in black (this study). Red beachballs represent earthquakes with inverse focal mechanisms, while blue beachballs represent those with normal focal mechanisms, and gray circles represent earthquakes without a focal mechanism, according to the ISC-GEM catalog (Storchak et al., 2013, 2015; Di Giacomo et al., 2018), chosen for its higher accuracy in epicentral locations. Black stars denote subduction earthquakes with $M_w > 7$. Inverted triangles represent seismic stations used for the seismic sequence analysis. The RSN (INSIVUMEH, 1976) is represented by yellow inverted triangles (with the letter A indicating the ATTAC project and the letter V indicating V-DAP, see description in the text), while seismic stations from Mexico, El Salvador, and Honduras are represented by green inverted triangles. Red arrows indicate the convergence velocities of the Cocos plate relative to the Central America forearc sliver, according to Ellis et al. (2019).

3 Seismicity associated with the M_w 6.2 earthquake

During the initial 25 days, more than 275 aftershocks were recorded and located using the SeisAn software

(Havskov and Ottemoller, 1999), with magnitudes ranging from 2.4 to 4.7. These aftershocks were dispersed throughout the vicinity of the mainshock, with their epicenters aligned in a NNE-SSW orientation. The main-

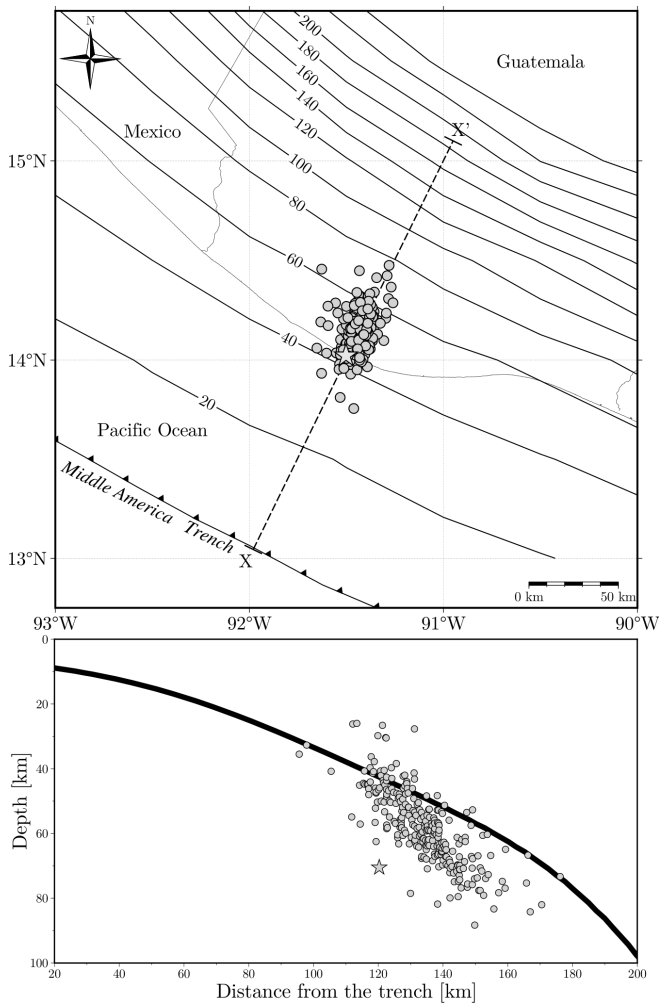


Figure 2 Geographic distribution and profile section (along X-X') of the preliminary main earthquake location (gray star) and the subsequent aftershocks sequence (gray dots). The slab model for the region is presented according to Hayes et al. (2018). The majority of earthquakes are situated at depths ranging from 40 to 80 km.

shock’s hypocenter was estimated to be at a depth of 70 ± 7 km, surpassing the Slab2 model’s approximate 50 km depth for that location (Hayes et al., 2018). Prior to the relocation process, the initial distribution of aftershock depths spanned from 40 to 80 km (Figure 2).

The CMT for the M_w 6.2 earthquake was derived using the W phase algorithm (Kanamori and Rivera, 2008; Hayes et al., 2018; Duputel et al., 2012). This solution incorporated data from the aforementioned seismic agencies as well as waveforms acquired through the Wilber 3 platform of the Incorporated Research Institutions for Seismology (Newman et al., 2013). The centroid depth was determined to be 60.5 km (Figure 4). The outcomes of the inversion process are presented in Table 1, allowing for a comparison with the results from the Global Centroid-Moment-Tensor Project (Dziewonski et al., 1981; Ekström et al., 2012) and the Advanced National Seismic System (ANSS) of the USGS.

Additionally, 12 focal mechanisms were estimated for the largest magnitude aftershocks using the P-wave first-arrival polarity method. The focal mechanisms obtained showed dominant normal and in-

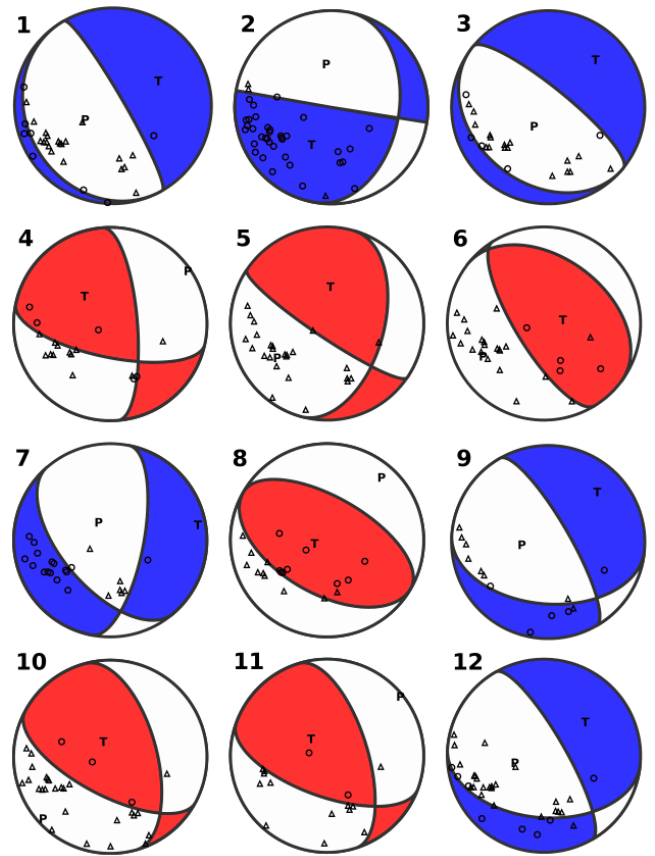


Figure 3 Focal mechanisms of the most significant aftershocks within the seismic sequence associated with the M_w 6.2 earthquake, determined using the first-arrival polarities method. Compression polarities are represented by circles, while dilation polarities are denoted by triangles. Events 1, 2, 3, 7, 9 and 12 exhibit larger components of normal focal mechanism, whereas events 4, 5, 6, 8, 10 and 11 display characteristics of inverse focal mechanism. P and T correspond to the pressure and tension axes, respectively.

verse components (Figure 3). The SeisAn software (Havskov and Ottemoller, 1999) was utilized, employing the FOCMEC (Snoke, 2003) and FPFIT (Reasenber and Oppenheimer, 1985) algorithms for this analysis.

3.1 Hypocentral relocation

We used the HypoDD v1.3 software in order to obtain a catalog of relocated seismic events (Waldhauser and Ellsworth, 2000; Waldhauser, 2001), which is a simultaneous relocation algorithm that minimizes the residual between observed and theoretical travel time differences (or double differences) for pairs of earthquakes recorded at each station while linking all observed event-station pairs (Waldhauser and Ellsworth, 2000). The Double-Differences technique takes advantage of the fact that if the hypocentral separation between two earthquakes is small compared to the event-station distance, then the ray paths between the source region and a common station are similar over almost the entire path (Fréchet, 1985; Got et al., 1994). In this case, the difference in travel times for two events observed at one station can be attributed to spatial shifting between the events with high precision. This approach

Agency	NP1	NP2	M_w	Centroid Depth (km)	Moment (N-m)
INSIVUMEH	182.6/ 34.0/ -14.9	285.1/ 81.7/ -123.1	6.24	60.5	2.85e+18
GCMT	189.2/ 49.2/ -10.6	286.2/ 82.0/ -138.7	6.20	63.5	2.41e+18
USGS	190.0/ 49.0/ -14.0	289.0/ 79.0/ -138.0	6.17	60.5	2.30e+18

Table 1 Comparison of the moment tensor's elements obtained in the present work with those of gCMT and USGS.

is especially useful in regions with a dense seismicity distribution (Waldhauser, 2001).

HypoDD calculates travel times in a layered velocity model for the current hypocenters at the station where the phase was recorded. Travel time differences are formed to link together all possible pairs of locations for which data is available. HypoDD solves for hypocentral separation after insuring that the network of vectors connecting each earthquake to its neighbors has no weak links that would lead to numerical instabilities.

For this, we built links from each event within a search radius of 8.0 km. We also required, at least, six links for each earthquake to form a neighborhood. With the network of phase pairs thus formed and using the local velocity model (INSIVUMEH, 1988), we obtained a relocated catalog with 234 events. Although the local velocity model is a 1D parallel layer model, HypoDD reduces the bias in locating individual events.

The results presented in Figure 4 show a significant clustering of earthquakes just beneath the upper part of the slab suggested by Hayes et al. (2018). This arrangement confines the depth of the majority of earthquakes to a range between roughly 50 and 65 km, with a handful of events reaching depths nearing 70 km, which includes the mainshock. Post-relocation, the mainshock was integrated into the sequence, although its depth was only slightly reduced to 69 km. As per the relocated catalog, the dimensions of the fault spanned $\sim 16 \text{ km} \times 22 \text{ km}$, corresponding to an approximate area of 350 km^2 .

3.2 Rupture plane and temporal evolution of seismicity

Based on the catalog of relocated earthquakes, the initial days showed concentrated seismic activity in a limited region with a subvertical orientation. As the seismic activity progressed, additional earthquakes were recorded both within this same area and further away, near the top of the slab, as depicted in Figure 5.

The estimated moment tensor analysis indicates that NP2 in Table 1 represents the primary rupture plane, where the majority of seismicity is distributed, as illustrated in Figure 6. Additionally, focal mechanisms with the highest normal component were found in the vicinity of this fault plane (blue beach balls in Figure 6), while focal mechanisms with the highest inverse components were observed in the upper region of the seismic activity (red beach balls in Figure 6).

3.3 Discussion and conclusions

The hypocenter's location at 69 km and the centroid's position at approximately 60 km (Figures 5 and 6) suggest that the rupture might have propagated from the LSL to the USL in the region of the estimated

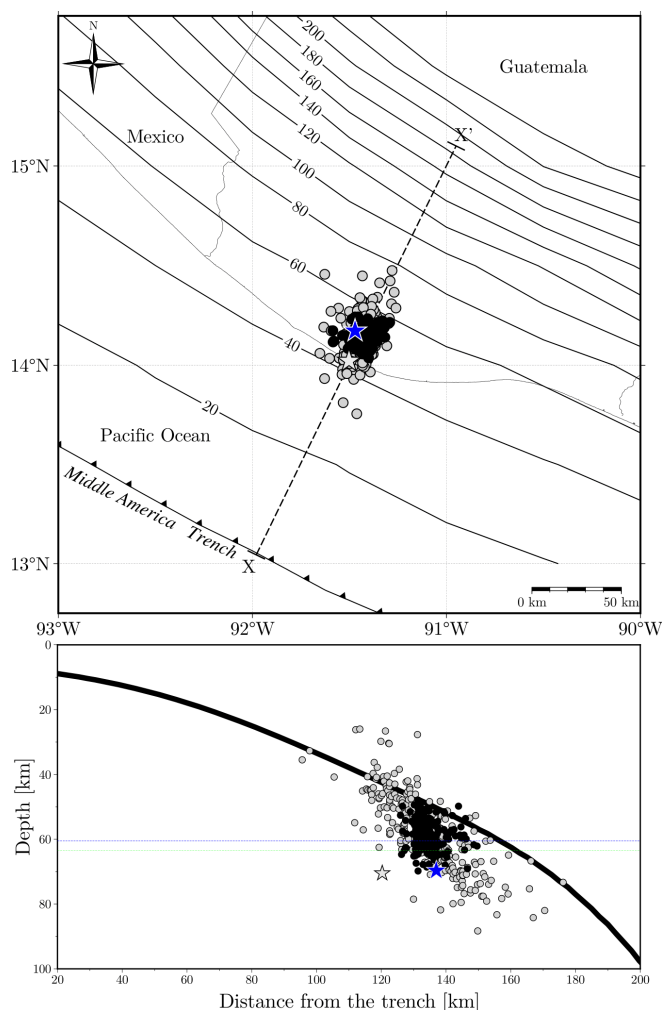


Figure 4 Comparison contrasting the initial positioning of the mainshock and the subsequent aftershock sequence (represented by the grey star and dots) with their subsequent relocation (indicated by the blue star and black dots), accomplished using the HypoDD technique (Waldhauser and Ellsworth, 2000; Waldhauser, 2001). The profile is along X-X' and the model of the top of the slab is according to Hayes et al. (2018). The horizontal dotted lines in the profile denoting the centroid depth reported by different agencies (blue line: INSIVUMEH, USGS; green line: gCMT. See Table 1).

plane. Rupture planes for earthquakes between the LSL and the USL have been documented for some large-magnitude intermediate-depth earthquakes (Twardzik and Ji, 2015), identified through associated aftershocks: the 2014 M_w 7.9 earthquake in Rat Islands, Alaska (Twardzik and Ji, 2015), the 2005 M_w 7.7 earthquake in Tarapaca, Chile (Peyrat et al., 2006; Delouis and Legrand, 2007), the 1993 M_w 7.6 Koshiro-Oki earthquake in Japan (Ide and Takeo, 1996), and the 2017 M_w 8.2 earthquake in Tehuantepec, Mexico, where two parallel

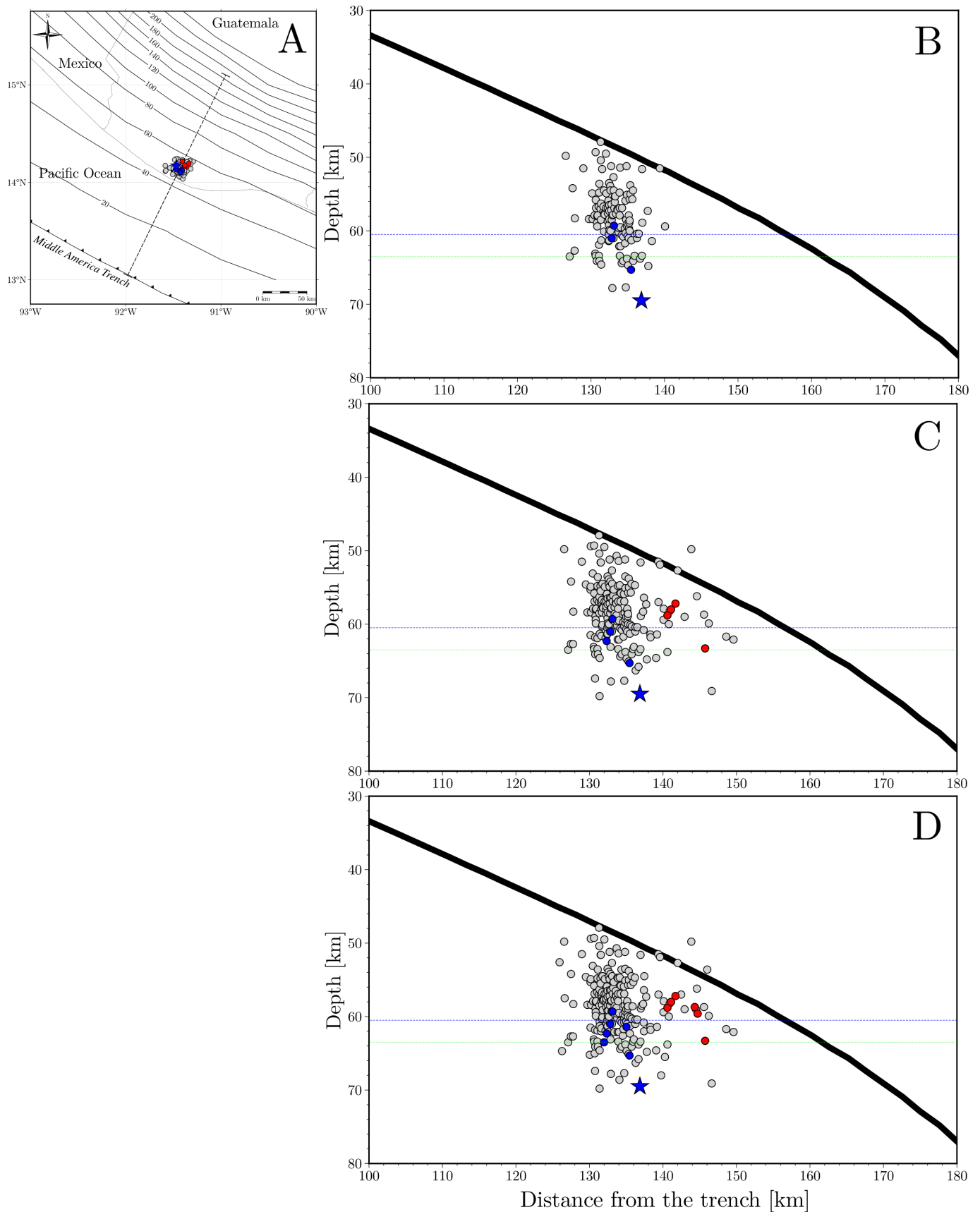


Figure 5 (A) Map of the relocated seismic sequence and profiles showing the temporal evolution of this seismicity in 5 days (B), 15 days (C) and 25 days (D). In the first interval (A), the earthquakes are distributed mainly in the region of the fault, while in the later intervals (B) and (C), hypocenters far from it can also be seen. The blue dots represent the earthquakes with normal focal mechanisms located in the main region of activity, while the red dots represent inverse focal mechanisms located near the upper region of the slab. The blue star represents the nucleation point and the horizontal dotted lines in the profile denoting the centroid depth reported by different agencies (blue line: INSIVUMEH, USGS; green line: gCMT. See Table 1).

faults were identified within the slab (SSN, 2017; Suárez et al., 2019). The dip angle of these earthquakes planes varies considerably.

In the Chilean subduction zone, moderate-magnitude earthquakes have been reported, and their rupture planes have been described through registered aftershocks. Marot et al. (2012) detailed the rupture plane of a M_w 5.7 earthquake that occurred in January 2003 in Central Chile, while Cabrera et al. (2021) identifies a fault plane for a M_w 6.3 earthquake in the northern region of the country that happened in October 2017.

As mentioned earlier, it is evident that most of the seismicity was generated in the region of the suggested plane, especially in the initial days of activity. However, later on, more dispersed seismicity is observed, with depths closer to the top of the slab, possibly in the USL (Figures 5 and 6). This scenario, where the seismicity generated by a normal earthquake triggers seismicity with inverse focal mechanisms, was also observed in the M_w 8.2 earthquake in Tehuantepec, Mexico (Ortega et al., 2019) and the M_w 5.7 earthquake in Central Chile (Marot et al., 2012). Chu and Beroza (2022) propose that intermediate-depth aftershocks are enabled by stress transfer and pore fluid redistribution in the proximity of the mainshock, which is enabled by dehydration. In our case, due to the proximity between the mainshock's fault plane and the USL, it is possible that such effects extend to that region, triggering seismic activity with a different rupture mechanism.

As shown in Figure 1, several intermediate-depth earthquakes with normal focal mechanisms have been documented in MGESZ (Storchak et al., 2013, 2015; Di Giacomo et al., 2018), similar to the M_w 6.2 earthquake analyzed in this study. However, this is the first instance where the fault plane has been identified through associated aftershocks, along with the triggering of seismicity outside the mainshock's rupture surface with a different focal mechanism.

Despite the fact that the sequence of earthquakes described was triggered by the M_w 6.2 earthquake, this zone had exhibited constant seismic activity (relative to the rest of the MGESZ region) before 16 February 2022, and continued in the subsequent months. Background seismicity in the area of the seismic sequence analyzed in this study can be seen in Figure 7, primarily with magnitudes less than four. Some earthquakes with magnitudes greater than five are notable. In mid-2021, a seismic swarm occurred, although no earthquake of significant magnitude was recorded. This behavior is possibly linked to dehydration processes within the slab (Kiser et al., 2011; Chu and Beroza, 2022) in this region (e.g., Pasten-Araya et al., 2018) but the data is inconclusive, and this explanation falls outside the scope of this work.

Although the estimated area with the sequence of relocated aftershocks covers an area of ~ 350 km², empirical relationships following Wells and Coppersmith (1994) suggest that the rupture area for a M_w 6.2 earthquake would extend to 170 km², about half of the area covered by the sequence. Furthermore, the estimate of 22 km fault length penetrating the slab aligns with the minimum value of 20 km reported by Ranero

et al. (2003) through seismic reflection data for bending-related faulting in the incoming plate at the Middle America trench. Therefore, it is possible that the main event triggered seismicity on a pre-existing fault, generated on the outer rise (Ranero et al., 2005; Kiser et al., 2011; Marot et al., 2012), also triggering out-of-plane seismicity.

This seismicity outside the fault plane includes the inverse earthquakes of the Figures 5 and 6, possibly occurring in the USL. Assuming that the nucleation of the mainshock occurred in the LSL, we can estimate an average separation between the LSL and USL of 12.2 ± 5.0 km (considering the estimated errors for preliminary hypocenter depth calculations and assigning a 10% error for values taken from Slab 2), consistent with previous estimates, particularly with Florez and Prieto (2019), confirming the trend of several double subduction zones with normal focal mechanisms in the LSL and inverse mechanisms in the USL (Craig et al., 2022; Chu and Beroza, 2022).

Acknowledgements

The support of the Swiss Agency for Development and Cooperation (SDC), the Swiss Seismological Service (SED) at ETH Zurich and the Volcano Disaster Assistance Program (VDAP) of the US Geological Survey (USGS), have been important for the expansion of the RSN and the improvement of the information generated by the INSIVUMEH. We want to express our sincere gratitude to Beatriz Cosenza, Marco Guzmán, and Xyoli Pérez for their valuable suggestions to the original manuscript of this work. Thanks to Gabriela Xol and Jorge Cárcamo for reviewing some of the data used.

Data and code availability

The HypoDD software (<https://www.ldeo.columbia.edu/felixw/hypoDD.html>) was used within the SeisAn software (<http://seisan.info/>). The preliminary and relocated catalogs, information about seismic stations, as well as the configuration and input files for the relocation can be found at: <https://zenodo.org/doi/10.5281/zenodo.8433469>.

For the inversion of W Phase, stations of the following seismic networks were also used: Caribbean Network (CU; doi: 10.7914/SN/CU), GEOFON (GE; doi: 10.14470/TR560404), Global Seismograph Network - IRIS/IDA (II; doi: 10.7914/SN/II), Mexican National Seismic Network (MX; doi: 10.21766/SSNMX/SN/MX), Nicaraguan Seismic Network (NU; doi: 10.7914/SN/NU), Servicio Nacional de Estudios Territoriales, El Salvador (SV; <https://www.fdsn.org/networks/detail/SV/>). We used the ISC-GEM Earthquake Catalogue (<https://doi.org/10.31905/d808b825>).

For the generation of maps we used QGIS V. 2.14.11 ESSEN (<https://qgis.org/en/site/forusers/download.html>) and GMT V. 6.4.0 (Wessel et al., 2019).

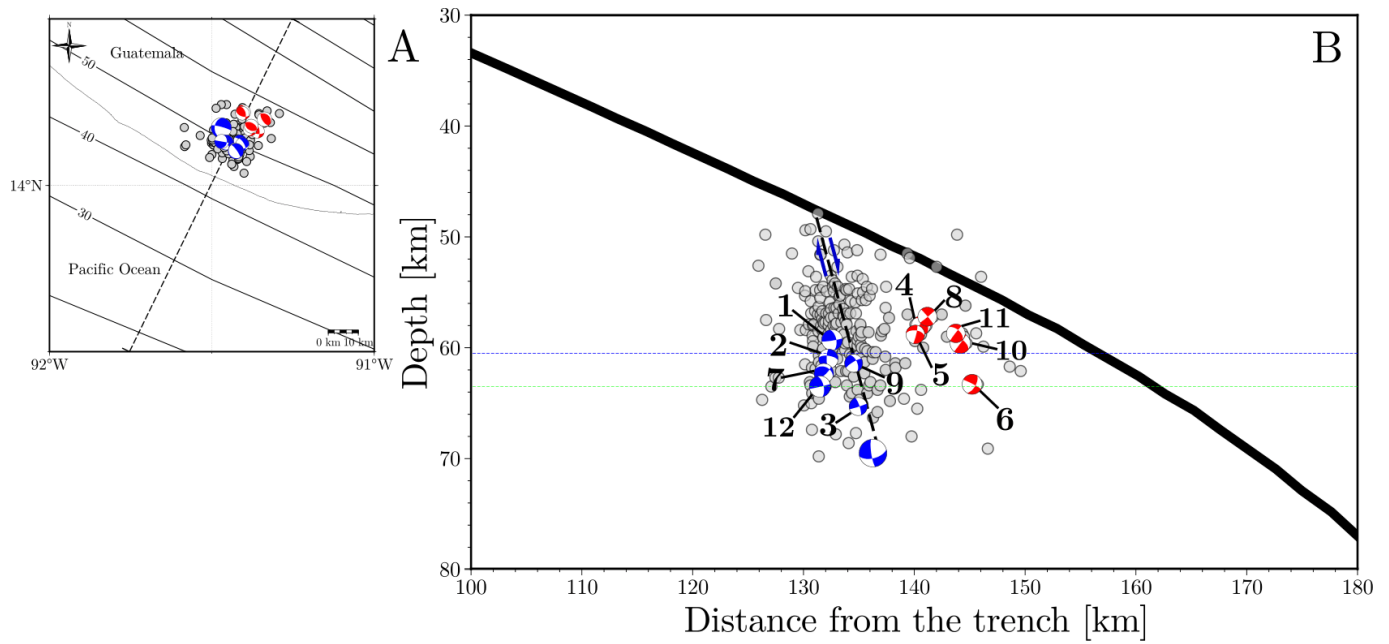


Figure 6 (A) Relocated seismic sequence (grey dots), blue beach balls are earthquakes with normal focal mechanisms located in the main region of activity, while red beach balls are inverse focal mechanisms located near the upper region of the slab as can be seen in profile (B). The numbering corresponds to Figure 3 and the focal mechanism of the M_w 6.2 earthquake is at the nucleation point. The dashed black line (approximately 22 km in length) in profile, shows the rupture plane with a dip angle as described for NP2 in Table 1 and the blue arrows represents normal fault movement. The horizontal dotted lines in the profile denoting the centroid depth reported by different agencies (blue line: INSIVUMEH, USGS; green line: gCMT. See Table 1).

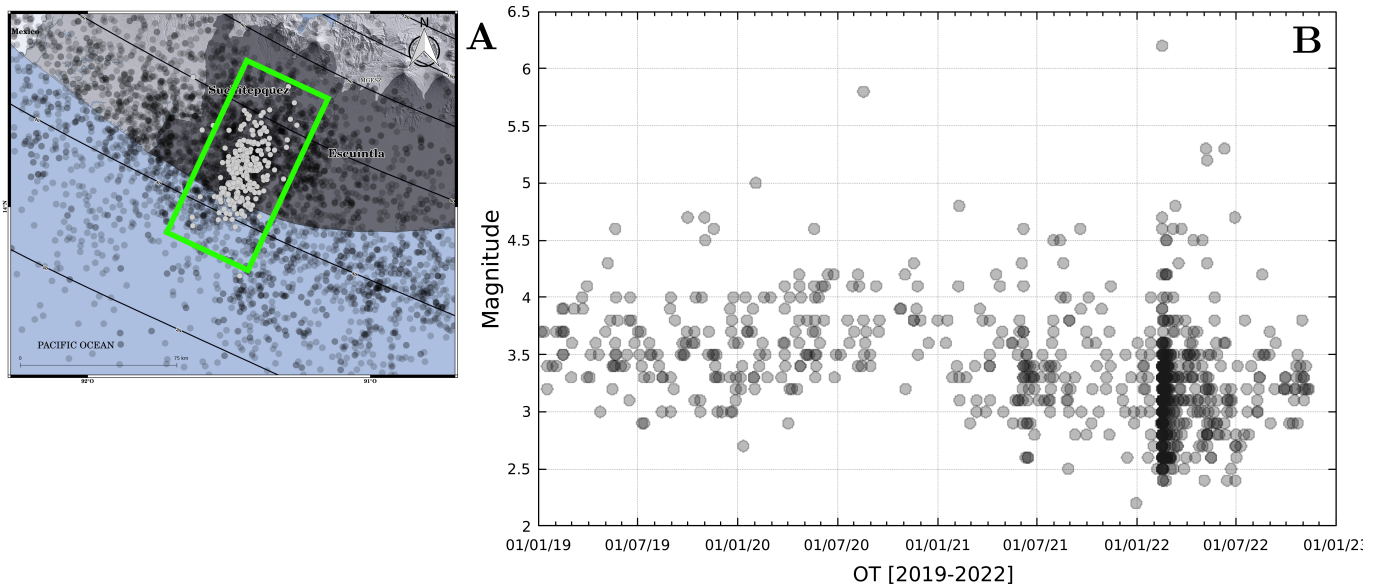


Figure 7 (A) Seismicity recorded by the RSN of INSIVUMEH from 2019 to 2022 on the southwest coast of Guatemala, the green square outlines the area where the sequence analyzed in this study occurred (before relocation). The temporal distribution of all seismic activity within that area is shown in (B). The horizontal axis displays the origin time (OT), and the magnitude is represented on the vertical axis. Earthquakes are depicted with transparent gray circles, where darker shades indicate a higher concentration of seismic events. Seismic activity has remained constant in the area, including some earthquakes with a magnitude greater than 5 and a seismic swarm in 2021. It is possible to observe an improvement in the RSN's ability to detect smaller magnitude earthquakes starting from 2021.

Competing interests

The authors have no competing interests.

References

Alvarez, J. Tectónica Activa y Geodinámica en el Norte de Centro América. *Universidad Complutense de Madrid*, Tesis Doctoral: 121–123, 2009.
 Ambraseys, N. and Adams, R. Large-magnitude Central Ameri-

- can earthquakes, 1898-1994. *Geophysical Journal International*, 127:665–692, Feb. 1996.
- Brudzinski, M., Thurber, C., Hacker, B., and Engdahl, R. Global Prevalence of Double Benioff Zones. *Science*, 316:1472–1474, June 2007. doi: 10.1126/science.1139204.
- Cabrera, L., Ruiz, S., Poli, P., Contreras-Reyes, E., Osses, A., and Mancini, R. Northern Chile Intermediate-Depth Earthquakes Controlled by Plate Hydration. *Geophysical Journal International*, 226:78–90, July 2021. doi: 10.1093/gji/ggaa565.
- Chu, S. X. and Beroza, G. C. Aftershock productivity of intermediate-depth earthquakes in Japan. *Geophysical Journal International*, 230(1):448–463, 01 2022. doi: 10.1093/gji/g-gac024.
- Craig, J., Methley, P., and Sandiford, D. Imbalanced Moment Release Within Subducting Plates During Initial Bending and Unbending. *Journal of Geophysical Research: Solid Earth*, 127, Feb. 2022. doi: 10.1029/2021JB023658.
- Delouis, B. and Legrand, D. M_w 7.8 Tarapaca intermediate depth earthquake of 13 June 2005 (northern Chile): Fault plane identification and slip distribution by waveform inversion. *Geophysical Research Letters*, 34, Jan. 2007. doi: 10.1029/2006GL028193.
- Di Giacomo, D., Engdahl, E. R., and Storchak, D. A. The ISC-GEM Earthquake Catalogue (1904–2014): status after the Extension Project. *Earth System Science Data*, 10(4):1877–1899, 2018. doi: 10.5194/essd-10-1877-2018.
- Duputel, Z., Rivera, L., Kanamori, H., and Hayes, G. W phase source inversion for moderate to large earthquakes (1990–2010). *Geophysical Journal International*, 189:1125–1147, May 2012. doi: 10.1111/j.1365-246X.2012.05419.x.
- Dziewonski, A., Chou, T., and Woodhouse, J. Determination of earthquake source parameters from waveform data for studies of global and regional seismicity. *Journal of Geophysical Research*, 86:2825–2852, Apr. 1981. doi: 10.1029/JB086iB04p02825.
- Ekström, G., Nettles, M., and Dziewoński, A. The global CMT project 2004-2010: Centroid-moment tensors for 13,017 earthquakes. *Physics of the Earth and Planetary Interiors*, 200-201:1–9, June 2012. doi: 10.1016/j.pepi.2012.04.002.
- Ellis, A., DeMets, C., McCaffrey, R., Briole, P., Cosenza, B., Flores, O., Graham, S., Guzmán-Speziale, M., Hernández, D., Kostoglodov, V., LaFemina, P., Lord, N., Lasserre, C., Lyon-Caen, H., Rodriguez, M., McCaffrey, R., Molina, E., Rivera, J., Rogers, R., and Staller, A. GPS constraints on deformation in northern Central America from 1999 to 2017, Part 1 – Time-dependent modelling of large regional earthquakes and their post-seismic effects. *Geophysical Journal International*, 214(214):2177–2194, June 2018. doi: 10.1093/gji/ggy249.
- Ellis, A., DeMets, C., McCaffrey, R., Briole, P., Cosenza, B., Flores, O., Guzmán-Speziale, M., Hernández, D., Kostoglodov, V., LaFemina, P., Lord, N., Lasserre, C., Lyon-Caen, H., Rodriguez, M., Molina, E., Rivera, J., Rogers, R., Staller, A., and Tikoff, B. GPS constraints on deformation in northern Central America from 1999 to 2017, Part 2: Block rotations and fault slip rates, fault locking and distributed deformation. *Geophysical Journal International*, 218:729–754, Apr. 2019. doi: 10.1093/gji/ggz173.
- Florez, M. A. and Prieto, G. A. Controlling Factors of Seismicity and Geometry in Double Seismic Zones. *Geophysical Research Letters*, 46, 2019. doi: 10.1029/2018GL081168.
- Fréchet, J. Sismogenèse et doublets sismiques. *Thèse d'Etat, Université Scientifique et Médicale de Grenoble*, 1985.
- Got, J., Fréchet, J., and Klein, F. Deep fault plane geometry inferred from multiplet relative location beneath the south flank of Kilauea. *Journal of Geophysical Research*, 99(B8):15375–15386, Aug. 1994. doi: 10.1029/94JB00577.
- Guzmán-Speziale, M. and Molina, E. Seismicity and seismically active faulting of Guatemala: A review. *Journal of South American Earth Sciences*, 115:103740, Feb. 2022. doi: 10.1016/j.jsames.2022.103740.
- Guzmán-Speziale, M. and Zúñiga, R. Differences and similarities in the Cocos-North America and Cocos-Caribbean convergence, as revealed by seismic moment tensors. *Journal of South American Earth Sciences*, 71:296–308, 2016. doi: 10.1016/j.jsames.2015.10.002.
- Güendel, F. and Protti, M. Sismicidad y Sismotectónica de América Central. *Física de la Tierra*, 10:19–51, 1998.
- Havskov, J. and Ottemoller, L. SeisAn Earthquake Analysis Software. *Seismological Research Letters*, 70(5):532–534, Sept. 1999. doi: 10.1785/gssrl.70.5.532.
- Hayes, G., Moore, G., Portner, D., Hearne, M., Flamme, H., Furtney, M., and Smoczyk, G. Slab2, a comprehensive subduction zone geometry model. *Science*, 362(6410):58–61, Oct. 2018. doi: 10.1126/science.aat4723.
- Ide, S. and Takeo, M. The dynamic rupture process of the 1993 Kushiro-oki earthquake. *Journal of Geophysical Research*, 101 (B3):5661–5675, Mar. 1996. doi: 10.1029/95JB00959.
- INSIVUMEH. Red Sismológica Nacional. *International Federation of Digital Seismograph Networks*, 1976. doi: 10.7914/SN/GI.
- INSIVUMEH. Boletín Sismológico 1983. *Instituto Nacional de Sismología, Vulcanología, Meteorología e Hidrología*, 1988.
- Kanamori, H. and Rivera, L. Source inversion of Wphase: speeding up seismic tsunami warning. *Geophysical Journal International*, 175:222–238, Oct. 2008. doi: 10.1111/j.1365-246X.2008.03887.x.
- Kiser, E., Ishii, M., Langmuir, C. H., Shearer, P. M., and Hirose, H. Insights into the mechanism of intermediate-depth earthquakes from source properties as imaged by back projection of multiple seismic phases. *Journal of Geophysical Research: Solid Earth*, 116(B6), 2011. doi: https://doi.org/10.1029/2010JB007831.
- Marot, M., Monfret, T., Pardo, M., Ranalli, G., and Nolet, G. An intermediate-depth tensional earthquake (M_w 5.7) and its aftershocks within the Nazca slab, central Chile: A reactivated outer rise fault? *Earth and Planetary Science Letters*, 327-328: 9–16, Apr. 2012. doi: 10.1016/j.epsl.2012.02.003.
- Newman, R., Clark, A., Trabant, C., Karstens, R., Hutko, A., Casey, R., and Ahern, T. Wilber 3: A Python-Django Web Application For Acquiring Large-scale Event-oriented Seismic Data. *Incorporated Research Institutions for Seismology*, Dec. 2013.
- Nishikawa, T. and Ide, S. Earthquake size distribution in subduction zones linked to slab buoyancy. *Nature Geoscience*, 7: 904–908, Dec. 2014. doi: 10.1038/NGEO2279.
- Ortega, R., Carciumaru, D., Quintanar, L., Huésca-Pérez, E., and Gutiérrez-Reyes, E. A Study of Ground Motion Excitation Based on the Earthquake of September 8, 2017: Evidence that Normal Faults Influence the Stress Parameter. *Pure and Applied Geophysics*, 176:1359–1377, Mar. 2019. doi: 10.1007/s00024-019-02150-2.
- Pasten-Araya, F., Salazar, P., Ruiz, S., Rivera, E., Potin, B., Maksymowicz, A., Torres, E., Villarroel, J., Cruz, E., Valenzuela, J., Jaldín, D., González, G., Bloch, W., Wigger, P., and Shapiro, S. A. Fluids Along the Plate Interface Influencing the Frictional Regime of the Chilean Subduction Zone, Northern Chile. *Geophysical Research Letters*, 45(19):10,378–10,388, 2018. doi: https://doi.org/10.1029/2018GL079283.
- Peyrat, S., Campos, J., de Chabaliér, J., Perez, A., Bonvalot, S., Bouin, M., Legrand, D., Necessian, A., Charade, O., Patau, G., Clévéde, E., Kausel, E., Bernard, P., and Vilotte, J. Tarapacá intermediate-depth earthquake (M_w 7.7, 2005, northern Chile): A slab-pull event with horizontal fault plane constrained from

- seismologic and geodetic observations. *Geophysical Research Letters*, 33, Nov. 2006. doi: 10.1029/2006GL027710.
- Ranero, C. R., Phipps Morgan, J., McIntosh, K., and Reichert, C. Bending-related faulting and mantle serpentinization at the Middle America trench. *Nature*, 425:367–373, 2003. doi: 10.1038/nature01961.
- Ranero, C. R., Villaseñor, A., Phipps Morgan, J., and Weinrebe, W. Relationship between bend-faulting at trenches and intermediate-depth seismicity. *Geochemistry, Geophysics and Geosystems*, 6(12), Dec. 2005. doi: 10.1029/2005GC000997.
- Reasenber, P. and Oppenheimer, D. Fpfit, fpplot, and fppage: Fortran computer programs for calculating and displaying earthquake fault plane solutions. *Technical report, USGS*, 1985.
- SNET. Servicio Nacional de Estudios Territoriales (SNET), El Salvador. 2004.
- Snoke, A. FOCMEC: FOcal MEchanism Determinations. *Virginia Tech*, Jan. 2003.
- SSN. Sismo de Tehuantepec (2017-09-07 23:49 M_w 8.2). *Servicio Sismológico Nacional, UNAM, Reporte Especial*, Nov. 2017.
- SSN. Servicio Sismológico Nacional, Instituto de Geofísica, Universidad Nacional Autónoma de México, México. 2022. doi: <https://doi.org/10.21766/SSNM/SN/MX>.
- Storchak, D., Di Giacomo, D., Engdahl, E., Harris, J., Bondár, I., Lee, W., Bormann, P., and Villaseñor, A. The ISC-GEM Global Instrumental Earthquake Catalogue (1900–2009): Introduction. *Physics of the Earth and Planetary Interiors*, 239:48–63, 2015. doi: <https://doi.org/10.1016/j.pepi.2014.06.009>.
- Storchak, D. A., Di Giacomo, D., Bondár, I., Engdahl, E. R., Harris, J., Lee, W. H. K., Villaseñor, A., and Bormann, P. Public Release of the ISC–GEM Global Instrumental Earthquake Catalogue (1900–2009). *Seismological Research Letters*, 84(5): 810–815, 09 2013. doi: 10.1785/0220130034.
- Suárez, G., Santoyo, M. A., Hjorleifsdottir, V., Iglesias, A., Villafuerte, C., and Cruz-Atienza, V. M. Large scale lithospheric detachment of the downgoing Cocos plate: The 8 September 2017 earthquake (M_w 8.2). *Earth and Planetary Science Letters*, 509:9–14, 2019. doi: <https://doi.org/10.1016/j.epsl.2018.12.018>.
- Twardzik, C. and Ji, C. The M_w 7.9 2014 intraplate intermediate-depth Rat Islands earthquake and its relation to regional tectonics. *Earth and Planetary Science Letters*, 431:26–35, Dec. 2015. doi: 10.1016/j.epsl.2015.08.033.
- Waldhauser, F. hypoDD – A Program to Compute Double-Difference Hypocenter Locations. *Open File Report USGS*, 2001.
- Waldhauser, F. and Ellsworth, W. A Double-Difference Earthquake Location Algorithm: Method and Application to the Northern Hayward Fault, California. *Bulletin of the Seismological Society of America*, 90(6):1353–1368, Dec. 2000. doi: 10.1785/0120000006.
- Wells, D. and Coppersmith, K. New Empirical Relationships among Magnitude, Rupture Length, Rupture Width, Rupture Area, and Surface Displacement. *Bulletin of the Seismological Society of America*, 84(4):974–1002, Aug. 1994. doi: 10.1785/BSSA0840040974.
- Wessel, P., Luis, J. F., Uieda, L., Scharroo, R., Wobbe, F., Smith, W. H. F., and Tian, D. The Generic Mapping Tools Version 6. *Geochemistry, Geophysics, Geosystems*, 20(11):5556–5564, 2019. doi: <https://doi.org/10.1029/2019GC008515>.
- White, R., Ligorria, J., and Cifuentes, I. Seismic history of the Middle America subduction zone along El Salvador, Guatemala, and Chiapas, Mexico: 1526–2000. *Geological Society of America, Special Paper* 375:379–396, 2004. doi: 10.1130/0-8137-2375-2.379.
- Ye, L., Lay, T., and Kanamori, H. Large earthquake rupture process variations on the Middle America megathrust. *Earth and Planetary Science Letters*, 381:147–155, 2013. doi: 10.1016/j.epsl.2013.08.042.

The article *The rupture plane of the 16 February 2022 M_w 6.2 Guatemala, intermediate depth earthquake* © 2023 by R. Yani-Quiyuch is licensed under CC BY 4.0.